Crystal fields at light rare-earth ions in Y and Lu

Touborg, P.; Nevald, Rolf; Johansson, Torben

Published in:
Physical Review B

Link to article, DOI:
10.1103/PhysRevB.17.4454

Publication date:
1978

Document Version
Publisher's PDF, also known as Version of record

Crystal fields at light rare-earth ions in Y and Lu

P. Touborg
Physics Department, University of Odense, 5000 Odense, Denmark

R. Nevald and T. Johansson
Department of Electrophysics, Technical University, 2800 Lyngby, Denmark

(Received 17 October 1977)

Crystal-field parameters have been deduced for the light rare-earth solutes Ce, Pr, and Nd in Y or Lu hosts from measurements of the paramagnetic susceptibilities. In the analysis all multiplets in the lowest *LS* term were included. For a given host, crystal-field parameters divided by Stevens factors B_{lm}/α_l, are of approximately the same magnitude for all the solutes Pr, Nd, Tb, Dy, Ho, Er, and Tm and do not scale with $\langle r^l \rangle$. The values deduced for Ce do not fit in with this simple picture. The higher-order parameters B_{40}, B_{60}, and B_{66} are, within the errors in their determination, identical in Y and Lu hosts, indicating that these values for a specific rare-earth solute in Y and Lu may give a reliable estimate for the corresponding sites in rare-earth metal. This is confirmed for Pr, for which these values and the value of B_{20} deduced from paramagnetic-susceptibility measurements on the pure metal, correctly explain the transition observed by neutron spectroscopy and the level crossing observed in a high-field experiment. A weighted average of B_{20} for cubic and hexagonal sites in Nd and Sm was obtained from the paramagnetic susceptibilities of these metals at high temperatures.

INTRODUCTION

In Ref. 1, the magnetic properties of dilute alloys of the rare-earth solutes Tb, Dy, Ho, Er, and Tm in the nonmagnetic hcp metal hosts Lu, Y, and Sc were reported and crystal-field parameters for all these systems deduced. The higher-order crystal-field parameters B_{40}, B_{60}, and B_{66} were observed to be rather insensitive to the host, the values being the same in Y and Lu and only slightly different in Sc. Due to the similarities of Y and Lu to the rare-earth metals, it was suggested that the value of these parameters in Y and Lu give a reliable estimate of the values in the magnetic rare-earth metals. B_{20} is host sensitive. The value of B_{20} in the magnetic rare-earth metals could be determined from the paramagnetic susceptibility of these metals measured up to high temperatures. For fixed host the crystal-field parameters divided by the Stevens factors, B_{lm}/α_l, seem to show a small variation with solute, but this does not follow the $\langle r^l \rangle$ variation with the radius of the solute $4f$ wave function predicted from simple theory.

To elucidate these results and also to determine the crystal-field parameters in the light rare-earth metals, we have studied dilute single-crystal alloys of the light rare-earth solutes Ce, Pr, Nd, and Sm in Lu and Y hosts, and also single crystals of pure Pr, Nd, and Sm in their paramagnetic phases.

A comparison between crystal-field parameters for light and heavy rare-earth solutes will clarify whether there is any variation with $4f$ radii of the solute (e.g., the ratios of $\langle r^2 \rangle$, $\langle r^4 \rangle$, $\langle r^6 \rangle$ for Pr to those for Ho are 1.6, 2.1, and 3.1, respectively[2]). Magnetic measurements in the paramagnetic range of the pure rare-earth metals can be related in a simple way to their crystal-field parameters. In the light rare-earth metal Pr, exchange interactions are small and Pr shows no ordering even at low temperatures.[3] Pr thus offers a unique opportunity to verify whether the parameters for dilute alloys are also representative for pure rare-earth metals. Furthermore, detailed information about the crystal fields in Pr is available from inelastic neutron diffraction[4] and high-field-magnetization measurements.[5]

We have performed susceptibility measurements on Pr, Nd, and Sm. Pr and Nd possess the double hcp (dhcp) structure and Sm possesses a rhombic structure. The dhcp structure and the Sm structure have lattice sites with both local hexagonal and—for ideal c/a ratio—local cubic symmetry. The values of B_{40}/β, B_{60}/γ, and B_{66}/γ, deduced from dilute alloys, may also be valid for the hexagonal sites in the pure metals, since these parameters are probably dominated by the local surroundings.

BASIC THEORY

The spin-orbit coupling in the light rare-earth metals is weaker than in the heavy rare-earth metals and the entire lowest *LS* term therefore has to be considered in accurate calculations of light rare-earth magnetic moments. (The inclusion of the higher-lying *J* multiplets gives a

correction of max ~3% for Pr, Nd, and Ce in the temperature ranges studied.) We thus work in the basis $|LM_L SM_S\rangle$, where L and S are the ground-term angular momentum quantum numbers given by Hund's rules. With this basis the Hamiltonian for a single rare-earth ion in the crystalline electric potential and in the applied magnetic field $\vec{H}$ has the general form

$$\mathcal{H} = \lambda \vec{L}\cdot\vec{S} + B_{20}^L O_2^0(\vec{L}) + B_{40}^L O_4^0(\vec{L}) + B_{60}^L O_6^0(\vec{L}) + B_{66}^L O_6^6(\vec{L}) + \mu_B(\vec{L}+2\vec{S})\cdot\vec{H} \quad (1a)$$

for hexagonal symmetry. The O_i^m are Stevens operators.[6] For ions on cubic sites we use the approximate Hamiltonian

$$\mathcal{H} = \lambda \vec{L}\cdot\vec{S} + B_{20}^L O_2^0(\vec{L}) + B_{40}^L [O_4^0(\vec{L}) - 20\sqrt{2}\, O_4^3(\vec{L})] + B_{60}^L [O_6^0(\vec{L}) + (35/\sqrt{8})O_6^3(\vec{L}) + \tfrac{77}{8} O_6^6(\vec{L})] + \mu_B(\vec{L}+2\vec{S})\cdot\vec{H}, \quad (1b)$$

where the form of the higher-order crystal-field terms is valid for perfect cubic symmetry. Exchange interactions, which are easily treated in the molecular-field model, have been omitted in (1a) and (1b). In the dilute alloys with Pr and Nd the molecular-field exchange parameters γ_a ($=\gamma_b$) and γ_c turned out to be neglectable (compare Ref. 1). For Y–8.7-at.% Ce and Pr crystal-field parameters were deduced in a way not affected by the exchange interactions, which are significant in these metals. The reduced matrix elements α_L, β_L, and γ_L entering as multiplicative factors when going from $\sum_i O_l^m(\vec{r}_i)$ to $O_l^m(\vec{L})$ are given in Table I. The relation between the crystal-field parameters B_{lm} used in Ref. 1 and the present parameters $B_l^L{}_m$ is $B_{20}^L/\alpha_L = B_{20}/\alpha$, etc. α, β, and γ are Stevens factors used in Ref. 1. Also included are the spin-orbit constants λ as calculated from the experimental energy splitting between the ground and first excited multiplets.[6]

For a given set of crystal-field parameters the zero-field susceptibility per atom in the direction of the applied field χ_H is calculated from the formula

$$\chi_H = \frac{\mu_B^2}{k_B T}\sum_n \sum_m{}' |\langle n|L_H + 2S_H|m\rangle|^2 \times e^{-E_n/k_BT}\Big/\sum_n e^{-E_n/k_BT} - 2\mu_B^2 \sum_n \sum_m{}'' |\langle n|L_H+2S_H|m\rangle|^2 (E_n - E_m)^{-1} \times e^{-E_n/k_BT}\Big/\sum_n e^{-E_n/k_BT}, \quad (2)$$

where $|n\rangle$, $|m\rangle$ and E_n, E_m are eigenfunctions and corresponding eigenvalues of the operator $\mathcal{H}_{H=0}$ in (1). The summation $\sum_m{}'$ is carried out over states $|m\rangle$ with $E_m = E_n$ and $\sum_m{}''$ over all other states. The zero-field susceptibility is isotropic in the basal plane.

TABLE I. Spin-orbit coupling constants and multiplicative factors for the light rare-earth metals studied.

	λ (K)	$10^{+2}\alpha_L$	$10^{+4}\beta_L$	$10^{+6}\lambda_L$
Ce	628.6	−4.444	40.40	−1036.00
Pr	604.8	−1.481	−3.848	24.67
Nd	497.4	−0.404	−1.224	−11.21
Sm	285.7	1.481	3.848	−24.67

The magnetic moment M_H per atom in the direction of the applied field is calculated from

$$M_H = \mu_B \sum_i \langle i|L_H + 2S_H|i\rangle e^{-W_i/k_BT}\Big/\sum_i e^{-W_i/k_BT}, \quad (3)$$

where $|i\rangle$ and W_i are eigenfunctions and eigenvalues of the entire operator in (1) and thus depend on $\vec{H}$.

For the structures with both hexagonal and cubic sites the susceptibility is calculated as a weighted average over the two types of sites ($\chi_{\text{dhcp}}^{(i)} = \frac{1}{2}\chi_{\text{cubic}}^{(i)} + \frac{1}{2}\chi_{\text{hex}}^{(i)}$; $\chi_{\text{Sm structure}}^{(i)} = \frac{1}{3}\chi_{\text{cubic}}^{(i)} + \frac{2}{3}\chi_{\text{hex}}^{(i)}$, $i = a$, b, or c).

RESULTS FOR DILUTE ALLOYS

Figures 1–5 show the experimental initial susceptibilities of Pr and Nd ions in Y and Lu and of Ce ions in Y, in the basal plane and along the c axis. The measurements were performed in fields up to 8×10^5 A/m (1T) using the Faraday method.[1] The data were determined from separate mea-

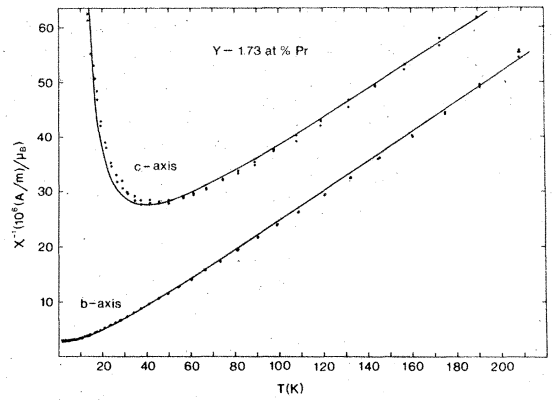

FIG. 1. Reciprocal initial susceptibilities of Pr in Y. The curves are calculated using the fitted parameters in Table II. In this and all subsequent figures, the theoretical curves are calculated with the assumption that $B_{66}^L/B_{60}^L = \frac{77}{8}$.

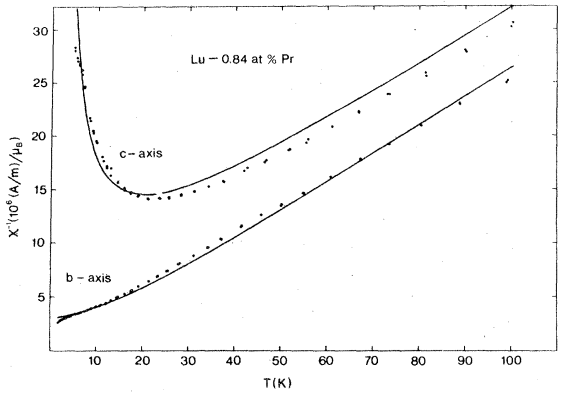

FIG. 2. Reciprocal initial susceptibilities of Pr in Lu. The curves are calculated using the fitted parameters in Table II.

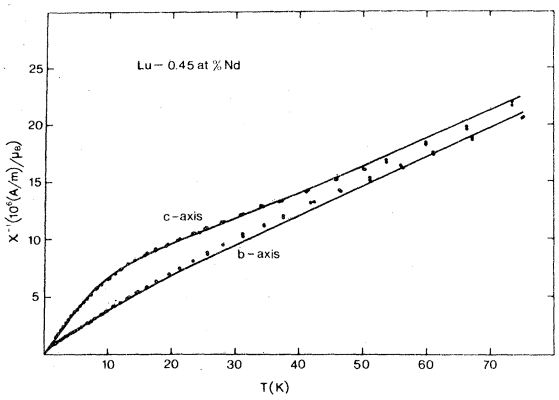

FIG. 4. Reciprocal initial susceptibilites of Nd in Lu. The curves are calculated using the fitted parameters in Table II.

surements of the susceptibilities of the alloy samples and of pure Y and Lu samples. The inaccuracies—which are mainly due to the irreproducibility of the susceptibilities of the host materials—are approximately 5% at the highest inverse susceptibility data in the figures. In order to obtain a reasonably accurate determination of the small susceptibilities of Ce and Sm solutes, rather concentrated (5%–10%) alloys had to be studied. For Sm alloys of this concentration the relatively large exchange interactions between Sm ions will cause ordering effects.

Preliminary measurements on an Y–2.73-at.%-Sm alloy showed susceptibilities of Sm of the same order of magnitude as for pure Sm in the paramagnetic phase. The susceptibilities were only slightly temperature dependent in the temperature range 20–200 K.

The experimental susceptibilities in Figs. 1–5 were analyzed using the Hamiltonian (1a). The parameters to be adjusted are B_{20}^L, B_{40}^L, B_{60}^L, B_{66}^L, and the concentration c. (Inclusion of exchange interactions in the molecular-field model did not change the fitted crystal-field parameters more than their final quoted uncertainties). The concentration is determined mainly from the slopes of the $1/\chi$ vs T curves at high temperatures. Evaporation of the rare-earth solute during the preparation of the alloy samples was detected in all cases.

The fitted crystal-field parameters are given in Table II. Crystal-field parameters with values in the ranges quoted in Table II reproduce the experimental susceptibilities within their uncertainties. As also found for heavy rare-earth solutes,[1] the fitted ratio B_{66}^L/B_{60}^L ($\equiv B_{66}/B_{60}$) for the Pr and Nd alloys is close to the value $\frac{77}{8}$ valid for ideal c/a ratio in the nearest-neighbor-superposition model.[7] For the Y-Ce alloy the effect on the susceptibilities of B_{60}^L and B_{66}^L is small (the

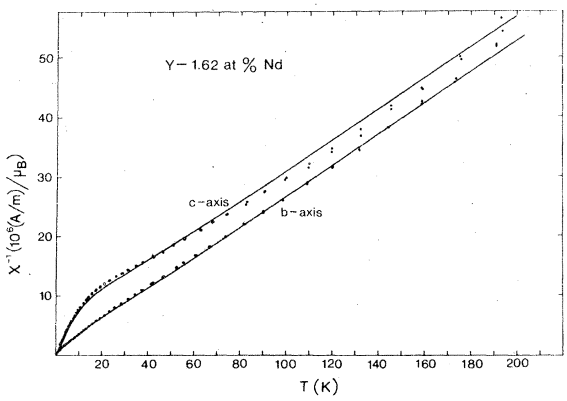

FIG. 3. Reciprocal initial susceptibilities of Nd in Y. The curves are calculated using the fitted parameters in Table II.

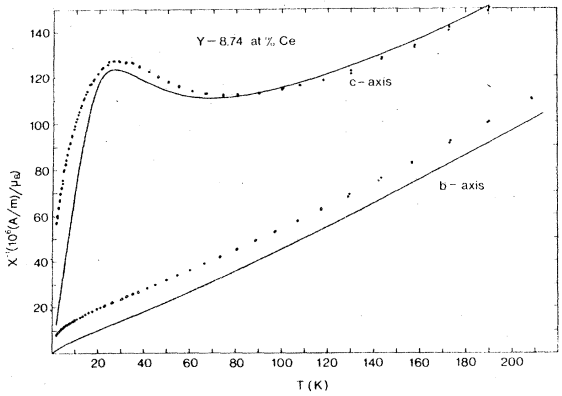

FIG. 5. Reciprocal initial susceptibilities of Ce in Y. The curves are calculated using the fitted values of B_{20}^L/α_L and B_{40}^L/β_L given in Table II and the arbitrary values B_{60}^L/γ_L = 22 K. (Exchange parameters $\gamma_c = \gamma_b = 0$.)

TABLE II. Values of fitted crystal-field parameters. B_{20}^L, B_{40}^L, and B_{60}^L are deduced for a fixed ratio $B_{66}^L/B_{60}^L = 77/8$. A simultaneous fit of B_{20}^L, B_{40}^L, B_{60}^L, and B_{66}^L/B_{60}^L gives approximately the same values of B_{20}^L, B_{40}^L, and B_{60}^L and the B_{66}^L/B_{60}^L values given in the table.

Alloy	B_{20}^L/α_L (K)	B_{40}^L/β_L (K)	B_{60}^L/γ_L (K)	B_{66}^L/B_{60}^L
Y–1.73-at.% Pr	−95 ± 10	4.0 ± 2	15.4 ± 1.5	10.6 ± 3
Lu–0.84-at.% Pr	−40 ± 7	5.0 ± 3	18.5 ± 1.5	10.3 ± 3
Y–1.62-at.% Nd	−90 ± 10	15.5 ± 6.5	22.0 ± 3	11.0 ± 2
Lu–0.45-at.% Nd	−32 ± 12	13.0 ± 6	23.5 ± 4.5	10.0 ± 2
Y–8.74-at.% Ce	−190 ± 30	−7.0 ± 5	•••	•••

effect vanishes, when higher-lying multiplets are neglected) and the parameters could not be determined uniquely from the measurements. Due to the exchange interactions present in the Y-Ce alloy (Fig. 5) the two parameters B_{20}^L and B_{40}^L were determined solely from the position in temperature of the maximum and minimum of the c-axis susceptibility. The susceptibilties of Ce in a Lu–2.6-at.%-Ce alloy showed the same general features as that of Y-Ce. The extrema in the c-axis susceptibility were, however, not sufficiently well defined to allow determination of the crystal-field parameters.

The parameters for Pr and Nd solutes resemble those for the heavy rare-earth solutes Tb, Dy, Ho, Er, and Tm (Figs. 3–5 in Ref. 1). For fixed host the parameters divided by the Stevens factors have approximately the same magnitude for all these seven solutes, although some variation with solute is observed. The higher-order parameters are the same in Y and Lu hosts, while B_{20} decreases with host in the order Y, Lu, (Sc).

Crystal-field parameters for Ce solutes have values significantly different from those for the other rare-earth solutes.

TABLE III. Crystal-field parameters for hexagonal sites in the light rare-earth metals. Within the uncertainty of its determination the parameter B_{66}^L has the value $77/8 \times B_{60}^L$. B_{20}^L/α_L for Nd and Sm is deduced from Figs. 9 and 10 assuming B_{20}^L/α_L to be identical on cubic and hexagonal sites, and assuming isotropic exchange. The parameters for Pr in parenthesis (from Ref. 14) are deduced from the excitation spectra for Pr and may include contributions from two-ion coupling.

Metal	B_{20}^L/α_L(K)	B_{40}^L/β_L(K)	B_{60}^L/γ_L(K)
Pr	−70 ± 25	4.3 ± 1.7	17.0 ± 1.1
	(−105 ± 22)	(9 ± 8)	(19 ± 2)
Nd	−32 ± 6	14.2 ± 4.4	22.5 ± 2.5
Sm	−90 ± 30	•••	•••

RESULTS FOR PURE METALS

As indicated by the results for the dilute alloys the values of B_{40}^L, B_{60}^L, and B_{66}^L for the hexagonal sites in Pr and Nd metals are expected to be similar to the values found when they are dissolved in Y and Lu (Table III). B_{20}^L is a host-sensitive parameter which may also be expected to depend on more distant neighbors in the lattice. This parameter therefore has to be derived from measurements on the pure rare-earth metals. B_{20}^L for the hexagonal sites in Pr can be extracted from the reciprocal initial susceptibilities shown in Fig. 6. The relatively high temperature, about 30 K, at which the minimum in the reciprocal c-axis susceptibility occurs, is expected to be approximately independent of exchange interactions. From this temperature, and the qualitative features of the susceptibility curves at higher temperature, the value of B_{20}^L for the hexagonal sites in Pr was extracted (Table III). All crystal-field parameters on the cubic sites were treated as unknown parameters. The illustrative curves

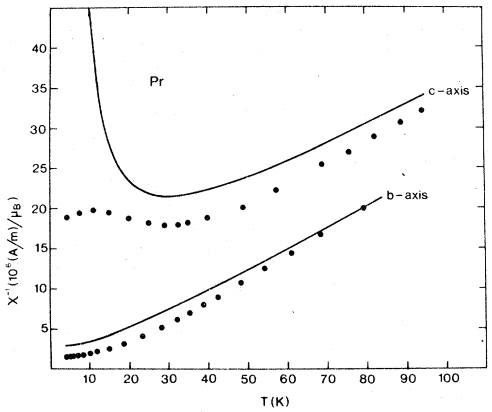

FIG. 6. Reciprocal initial susceptibilities of Pr. (Experimental data from Ref. 8.) The curves are calculated using the parameters given in Table III assuming identical parameters on cubic and hexagonal sites and neglecting exchange.

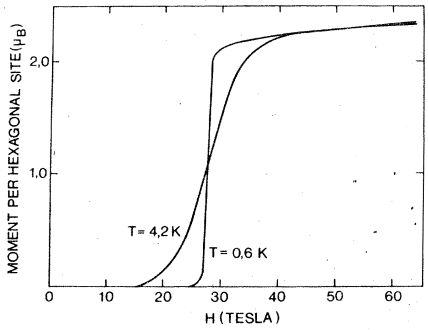

FIG. 7. Theoretical magnetization curves for hexagonal sites in Pr. The crystal-field parameters given in Table III and the exchange parameter $\gamma_c = 0$, have been used.

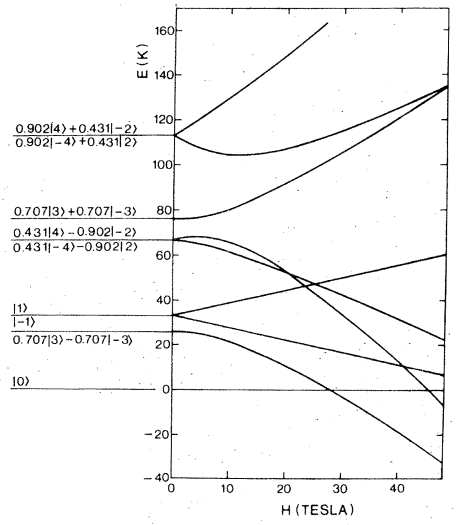

FIG. 8. Energy levels at zero field and as a function of field for ions on hexagonal sites in Pr. In the listing of wave functions, admixing of functions from higher-lying multiplets has been left out. Crystal-field parameters are given in Table III.

plotted in Fig. 6 are calculated using identical values of parameters for cubic and hexagonal sites and neglecting the exchange interactions.

It is generally accepted[4,5,9,10] that the four lowest states of Pr ions on the hexagonal sites are a singlet ground state $|M_J = 0\rangle$, a singlet mixed state $(1/\sqrt{2})(|3\rangle - |-3\rangle)$ and a doubly degenerate state $|\pm 1\rangle$. From the dispersion relation for magnetic excitations as determined by inelastic neutron scattering[4] it is deduced that the splitting between the states $|0\rangle$ and $|\pm 1\rangle$ is about 37 K.

Another aspect of particular interest is observed in the high-field magnetization measurement[5] along the c direction at 4.2 K: The magnetization increases smoothly by about $1\mu_B$ per 30 T and per atom but at 31.5 T it jumps abruptly by $1.04\mu_B$ per atom ($2.08\mu_B$ per hexagonal site). The smooth increase is believed to originate from ions on cubic sites, whereas the abrupt transition is attributed to the crossing at this field of an approximate $|-3\rangle$ state through the singlet ground state $|0\rangle$ for ions on hexagonal sites.

Applying the values in Table III, all the experimental data for the hexagonal sites in Pr are reproduced within the experimental uncertainties. The theoretical c-axis magnetization curves as a function of field for the hexagonal sites are shown in Fig. 7. These curves exhibit the same charac-

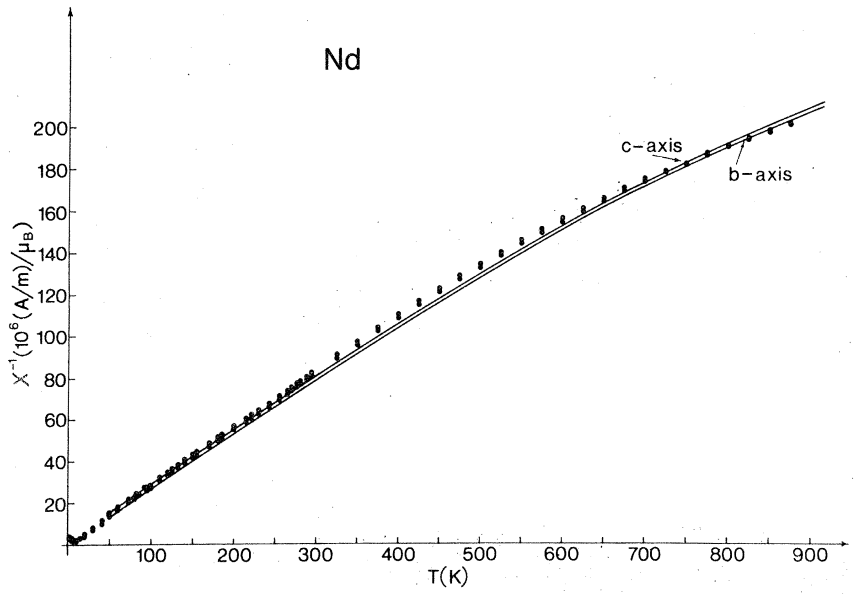

FIG. 9. Reciprocal initial susceptibilites of Nd. The curves are calculated using the parameters in Table III assuming identical parameters on cubic and hexagonal sites, and neglecting exchange.

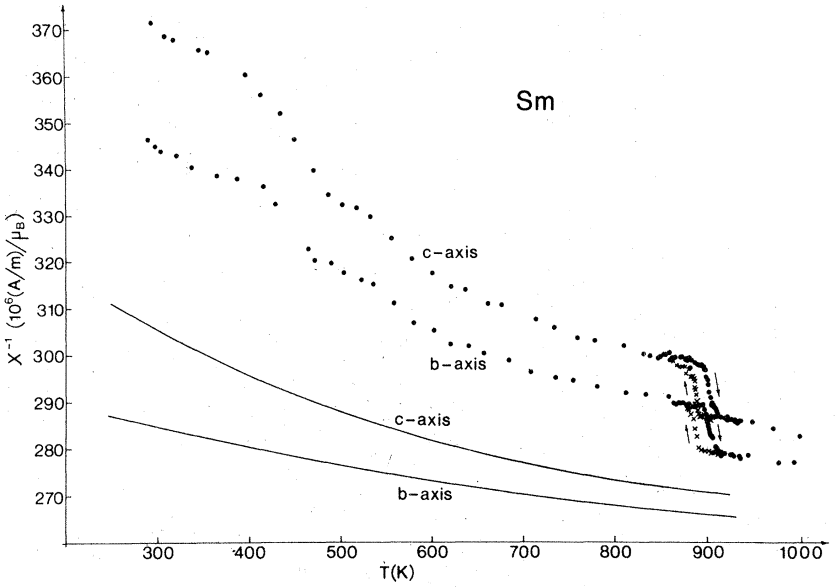

FIG. 10. Reciprocal initial susceptibilities of Sm. (Experimental data from Ref. 12.) The curves are calculated using the parameters $B_{20}^L/\alpha_L = -90$ K, $B_{40}^L/\beta_L = 6.8$ K and $B_{60}^L/\gamma_L = 13.6$ K, for both cubic and hexagonal sites, and neglecting exchange. The higher-order parameters used are average values for heavy rare-earth solutes in Y and Lu. Note the suppressed zero on the $1/\chi$ axis.

teristics as the experimental data. The jump is of the same magnitude and the experimental transition field at 31.5 T is reproduced within the parameter ranges given in Table III. (A change of B_{20}^L/α_L from 70 to 78 K shifts the transition field from 28 to 31.5 T.) The abrupt increase observed experimentally, in contrast to the continuous behavior in Fig. 7, cannot be reproduced theoretically without including exchange interactions.

Also, the theoretical energy level scheme (Fig. 8) for the hexagonal sites is consistent with the experimental evidence. The parameters in Table III predict a splitting of 33 ± 2 K between the $|0\rangle$ and $|\pm 1\rangle$ states at zero field. This agrees well with the experimental value of about 37 K. Within the uncertainty limits in Table III the order of the $|\pm 1\rangle$ doublet and the $(1/\sqrt{2})(|3\rangle - |-3\rangle)$ singlet in the level scheme is undetermined. Figure 8 also shows the energy levels as a function of field. The mixing in the field of the two states $|3\rangle + |-3\rangle$ and $|3\rangle - |-3\rangle$ changes the lower energy state continuously towards an approximate $|-3\rangle$ state, which crosses through the $|0\rangle$ ground state.

The susceptibility of Ce has not been studied, due to the severe difficulties in producing single crystals of this metal.[11] Figures 9 and 10 show high temperature susceptibilities of Nd and Sm. The magnetic ordering in Nd (below 19 K) and Sm (below 106 K) and the relatively featureless paramagnetic susceptibilities of these metals prevent a separate determination of B_{20} for the hexagonal sites. Assuming isotropic exchange, weighted-average values (Table III) of B_{20}/α_L for cubic and hexagonal sites can be extracted from Figs. 9 and 10. The effects of the higher-lying multiplets, especially on the Sm susceptibilities, are noteworthy. A crystallographic phase transition (Sm structure ↔ hcp or dhcp structure[13]) is revealed in the susceptibility data in Fig. 10.

CONCLUSION

We have determined the crystal fields acting on light rare-earth ions dissolved in Y and Lu and in some light rare-earth metals. For a fixed host the crystal-field parameters divided by Stevens factors, B_{lm}/α_l, are of approximately the same magnitude for Pr, Nd, Tb, Dy, Ho, Er, and Tm solutes and do not scale with $\langle r^l \rangle$. The crystal fields deduced for Ce do not fit in with this simple picture.

The higher-order parameters for Pr, Nd, and the heavy rare-earth metals are identical in Y and Lu hosts, indicating that these values may give a reliable estimate of the crystal-field anisotropy of the magnetic metals. Due to the relatively small strength of the exchange interactions in Pr, contributions from two-ion couplings to the anisotropy are expected to be small. The crystal-field parameters for Pr therefore agree with those determined from the excitation spectra for Pr (Table III) and give a satisfactory account of the experimental data for the hexagonal sites in Pr.

ACKNOWLEDGMENTS

The authors acknowledge fruitful discussions with Dr. J. Hǿg, Professor V. Frank, and Professor A. R. Mackintosh.

[1]P. Touborg, Phys. Rev. B 16, 1201 (1977).
[2]A. J. Freeman and R. E. Watson, Phys. Rev. 127, 2058 (1962).
[3]B. Lebech, K. A. McEwen, and P. A. Lindgård, J. Phys. C 8, 1684 (1975).
[4]J. G. Houman, M. Chapellier, A. R. Mackintosh, P. Bak, O. D. McMasters, and K. A. Gschneider, Jr., Phys. Rev. Lett. 34, 587 (1975).
[5]K. A. McEwen, G. J. Cock, L. W. Roeland, and A. R. Mackintosh, Phys. Rev. Lett. 30, 287 (1973).
[6]A. Abragam and B. Bleaney, *Electron Paramagnetic Resonance of Transition Ions* (Clarendon, Oxford, 1970).
[7]D. J. Newman, Adv. Phys. 20, 197 (1971).
[8]T. Johansson, K. A. McEwen, and P. Touborg, J. Phys. (Paris), Colloq. 32, C1-372 (1971).
[9]B. D. Rainford and J. Gylden Houman, Phys. Rev. Lett. 26, 1254 (1971).
[10]B. Lebech and B. D. Rainford, J. Phys. (Paris) 32, 370 (1971).
[11]K. A. McEwen and P. Touborg, J. Phys. F 3, 1903 (1973).
[12]P. Touborg and K. A. McEwen (unpublished).
[13]P. G. Mardon and C. C. Koch, Scr. Metall. 4, 477 (1970).
[14]J. Jensen, Physica B86–88, 32 (1977).